Air Quality, Atmosphere & Health
https://doi.org/10.1007/s11869-025-01738-z

COVID-19 pandemic impacted differently air quality in Latin American cities

Oliva Atiaga[1] · Fernando Páez[1] · Wilson Jácome[1] · Rafael Castro[2] · Edison Collaguazo[2] · Luís Miguel Nunes[3]

Received: 27 January 2025 / Accepted: 18 April 2025

Abstract

This research explores the spatial and temporal variations of nitrogen dioxide (NO_2), sulphur dioxide (SO_2), and ozone (O_3) levels in four Latin American cities, namely Mexico City, Santiago de Chile, Lima, and the Metropolitan District of Quito, utilizing Sentinel-5P satellite data alongside ground-based monitoring stations. The period covers pre-lockdown, lockdown, and post-lockdown phases of the COVID-19 pandemic, providing insights into pollutant behaviour across different levels of human activity. Findings show notable spatial variability in pollutant levels, with Santiago de Chile repeatedly presenting the highest concentrations of NO_2 and SO_2, linked to urban development and local weather patterns, whereas Quito showed the lowest levels. The lockdowns typically resulted in decreased NO_2 concentrations, yet their effects on SO_2 and O_3 levels were inconsistent, highlighting the complexity of pollutant interactions. The research confirms that satellite data serves as an affordable addition to conventional monitoring, especially in areas with limited resources. These results emphasize the necessity for customized, city-oriented strategies to reduce urban air pollution and safeguard public health.

Keywords Air quality · COVID-19 · Satellite data · Latin America

Introduction

Every year it is estimated that exposure to air pollution causes 7 million premature deaths in the world, and in 2019, more than 90% of the population lived in places where concentrations of pollutants exceed the values of the guidelines given by the World Health Organization (World Health Organization 2025).

This study focuses on cities located in Latin America, being population density one of the factors responsible for a significant amount of pollutants emitted into the atmosphere (Gómez Peláez et al. 2020). Thus, in Latin America and the Caribbean, the estimated population for 2022 was 664,419,700 people, equivalent to 8.42% of the world population, occupying the fourth place among the most populated regions in the world, and its population density is estimated that it has increased to 32.5 people per km^2 (United Nations 2019). On the other hand, cities such as Lima, Santiago de Chile and Mexico City, are among the cities that have the greatest road congestion and this is a growing problem in cities in Latin America, a problem aggravated by the possible post-pandemic increase in road use of private vehicles (Bedoya-Maya et al. 2022). In the specific case of Mexico City, although air pollution has decreased significantly in the last three decades, some of the pollutants, such as particulate matter (PM) and Ozone (O_3), are frequently above established air quality standards in Mexico (Vega et al. 2021). Besides, Santiago de Chile also constitutes an urban area with high pollution rates (Toro A. et al. 2021).

With respect to the city of Lima, Peru, this is the third most populated city and one of the most polluted in America, it is among the five most polluted urban centers in South America (Vu et al. 2021), being terrestrial transportation, one of the main contributors to atmospheric polluting emissions, due to its aging vehicle fleet (Vu et al. 2021) and with

✉ Luís Miguel Nunes
lnunes@ualg.pt

[1] Departamento de Ciencias de la Tierra y la Construcción, Universidad de las Fuerzas Armadas ESPE, Av. General Rumiñahui s/n, P.O. Box 171-5-231B, Sangolquí, Ecuador

[2] Geospace Solutions, Av. Manuel Córdova Galarza km 4.5, P.O. Box 170177, Quito, Ecuador

[3] Faculdade de Ciências e Tecnologia, Universidade do Algarve, CERIS, Campus de Gambelas, Faro, Portugal

Published online: 17 May 2025

a significant increase in vehicles between 2000 and 2014, that contributed to an increase of approximately 65% in emissions from the vehicles (Zalakeviciute et al. 2024). Besides, in the city of Lima, the dominant winds from the Pacific Ocean, push pollutants inward, where they are retained in the hills and mountains (Vu et al. 2021). While the Metropolitan District of Quito (DMQ), due to its irregular topography, disproportionately long and narrow, some parts are developed on steep slopes, while very limited parts are located on level terrain, air pollutants are produced, in a big extent, due to the emissions from vehicles, which heavily rely on fossil fuels. Such pollutants are basically accumulated in the lower zones of the city (Romero et al. 2020).

During the COVID-19 pandemic, lockdown measures were implemented around the world, which contributed to the variation in concentrations of the main regulated pollutants (Wang and Li 2021; Toro A. et al. 2021; Sahraei et al. 2021; Vega et al. 2021), such as: nitrogen dioxide (NO_2), sulfur oxide (SO_2), particulate matter (MP: MP10 and $MP_{2.5}$) and ozone (O_3) (Burns et al. 2020; Albayati et al. 2021). On the other hand, numerous studies show that air pollution can cause heart and lung disorders, reduced lung function, respiratory symptoms, and even premature deaths (Li et al. 2021; Albayati et al. 2021), and also such pollution is presumed to cause an increase of the rate of contracting a viral infection like COVID-19 (Albayati et al. 2021; Mathys et al. 2023).

Besides, emissions from transportation, industrial areas, natural emissions due to changes in land use, volcanic eruptions, forest emissions and biomass burning, are poorly quantified worldwide (Veefkind et al. 2012), therefore, satellite measurements, such as those from the Sentinel-5P satellite, provided by the Tropospheric Monitoring Instrument (TROPOMI), constitute a useful tool for establishing updated scenarios applied to environmental assessment, for the improvement of air quality and human health (Bodah et al. 2022) and has been key to understand the state of the air and its trends on a regional and global scale, providing information in the quantitative manner (Levelt et al. 2018), about the emissions and transport of pollutants.

Urban and population growth in Latin American countries, forces different governments to increase investment in their atmospheric monitoring networks; however, this is not possible for developing countries since they do not have the necessary economic resources. Therefore, it is pertinent that Latin American countries choose to use technologies that require less investment, such as satellite remote sensing. This method can be considered a complement to atmospheric monitoring with ground-level stations; since satellite measurements of the indicated pollutants are consistent in time and space; and also, the scope and scale of space-based Earth observations increasingly correspond to the needs of global health assessments (Anenberg et al. 2020).

Several studies have been carried out in cities in Latin America, in order to determine the effect of the lockdown, which was established as a measure to avoid COVID-19 infections, with data from ground monitoring stations and satellite data, or a combination of data, like the study case carried out in urban centers of Latin American countries for NO_2 concentrations, before and during lockdown, due to COVID-19 (March-June 2020) compared to the period (March-June 2019) (Volke et al. 2023), another study case was carried out in the urban area of Santiago de Chile (Toro A. et al. 2021), in which they compared data on concentrations of pollutants (PM_{10}, $PM_{2.5}$, NO_x, CO and O_3) from the period March to May 2020, with the average concentrations corresponding to the same period from 2017 to 2019. In the Lima Metropolitan Area (LMA), a study was carried out with data from the monitoring stations and satellite data, for PM_{10}, $PM_{2.5}$, NO_2 and O_3, during the months of February, March and April 2020, which were compared to data from the same months, for the period of 2017 to 2019 (Rojas et al. 2021). In the same way, in a study of some cities (Vega et al. 2021) in which Mexico City was included with data from the Automatic Atmospheric Monitoring Network (RAMA), for PM_{10}, $PM_{2.5}$, NO_2, CO and O_3, changes were evaluated for the period January 1 to August 31, 2020, with respect to average concentrations in the same period for 2017 to 2019. Other studies have been carried out which focus on the application of remote sensors as a complement to atmospheric monitoring with meteorological stations, mainly for $PM_{2.5}$ and NO_2 in several Latin American cities such as: Lima, Arequipa, Santiago de Chile, Guayaquil, Medellín, Cali, Bogotá, Barranquilla, Rio de Janeiro, Mexico City and Buenos Aires (Benchrif et al. 2021; Ray et al. 2022) Latin America, with its densely populated cities like Mexico City, Santiago, Lima, and Quito, reflects the air quality dynamics in developing economies, making these findings applicable to similar urban centers worldwide. The analysis of pollutant levels under varying socio-economic and meteorological conditions provides insights for global air quality management strategies.

We tested the hypotheses that air quality changes in Latin American cities due to COVID-19 mobility restrictions could be assessed using satellite data, and that these changes occurred both during and after the lockdowns.

For the aforementioned, the objectives of this work are: (1) Compare spatial-temporal concentrations of NO_2, SO_2 and O_3 in different cities in Latin America, with satellite data in three periods: before lockdown, during lockdown and after lockdown, for each city, and (2) Validate satellite data with data from monitoring stations.

Table 1 Geographic coordinates of the area limits and studied periods

Study Zones	Upper Left Geographic Coordinate		Lower Right Geographic Coordinate		Period		
	Longitude	Latitude	Longitude	Latitude	Pre Lockdown	Lockdown	Post Lockdown
Ciudad de México	-99.406724	19.743493	-98.861828	19.133242	December 2018 to February 2020	March 2020 to May 2020	June 2020 to December 2023
Lima	-77.210706	-11.816309	-76.821233	-12.251414	December 2018 to February 2020	March 2020 to June 2020	July 2020 to December 2023
Santiago de Chile	-70.895446	-33.235564	-70.392728	-33.711470	December 2018 to February 2020	March 2020 to July 2020	August 2020 to December 2023
DMQ	-78.994456	0.308595	-78.102158	-0.643189	December 2018 to February 2020	March 2020 to May 2020	June 2020 to December 2023

Table 2 Imagery collections and selected bands

Image name	Band name	Description	Resolution (m)	Units
COPERNICUS/S5P/OFFL/L3_NO2	tropospheric_NO2_column_number_density	tropospheric vertical column density	1113.2	mol/m^2
COPERNICUS/S5P/OFFL/L3_SO2	SO2_column_number_density	SO2 vertical column density at ground level	1113.2	mol/m^2
COPERNICUS/S5P/OFFL/L3_O3	O3_column_number_density	Total atmospheric column ozone concentration	1113.2	mol/m^2

The integration of Sentinel-5P satellite data and ground-based monitoring is a methodological advancement, enabling high-resolution assessments of NO_2, SO_2, and O_3 levels across time periods before, during, and after lockdowns. This dual approach helps confirm satellite measurements and also demonstrate their utility as a cost-effective alternative for air quality monitoring in resource-constrained regions.

Methodology

Study área and temporal period

The study was carried out in Latin American cities: Mexico, Lima, Santiago de Chile and the Metropolitan District of Quito (DMQ) (details are provided in Figure SM1). The study areas were defined by establishing regular geometric polygons, whose coordinates are presented in Table 1. In addition to monthly data analysis, study periods were established: before, during and after lockdown. The lockdown period was established according to the official decrees and resolutions issued in each country for the management and control of the COVID-19 pandemic (Table 1). The pre-lockdown period was established from December 2018 and the post-lockdown period was extended to December 2023, in order to determine long-term variations in air quality. The post lockdown period of over 40 months is expected to cover the full period necessary for the economic activity to return to the pre-pandemic condition (Brooks and Harris 2023).

Data collection and processing

Offline data pertaining to level 3 concentrations of nitrogen dioxide (NO_2), sulfur dioxide (SO_2), and ozone (O_3) [mol/m^2] were utilized in this study. These data were sourced from the Tropospheric Monitoring Instrument (TROPOMI) aboard the Sentinel-5P (S5P) satellite. Monthly averages were calculated for the period from December 2018 to December 2023, using Google Earth Engine (GEE) (Crosman 2021). The datasets provided by S5P are available in two versions: Near Real-Time (NRTI) and Offline (OFFL). NRTI data are made accessible within three hours following data acquisition, while OFFL data are available within a few days post-acquisition (Shikwambana et al. 2020). For the purposes of this research, we employed the collections Sentinel-5P OFFL NO2 - Offline Nitrogen Dioxide, Sentinel-5P OFFL SO_2 - Offline Sulfur Dioxide, and Sentinel-5P OFFL O_3 - Offline Ozone; additional information regarding these datasets is presented in Table 2. The original Sentinel 5P Level 2 (L2) data is binned by time, not by latitude/longitude. To make it possible to ingest the data into Earth Engine, each Sentinel 5P L2 product is converted to L3, keeping a single grid per orbit. In the case of vertical column densities of the NO2, the accuracy has been improved by using the 3-dimensional global TM5-MP chemistry transport model with a higher resolution than the 1×1 degree (Ialongo et al. 2020). On the other hand, due to the noise, there are some negative values of vertical columns for the SO2, in clean regions or low emissions of SO2, for which the atypical values were filtered out as concentration values lower than -0.001 mol/m2, which is recommended in the Earth Engine Data Catalog (https://developers.google.com

/earth-engine/datasets/catalog?hl=es-419). The data quality assessment was conducted using the harpconvert tool with the binspatial operation (Gorelick et al. 2017), which filters and excludes pixels that do not meet the quality assurance criteria (qa-value), thereby eliminating cloud contamination and other low-quality retrievals.

Additionally, the qa value was adjusted before running harpconvert to satisfy all of the following criteria: for the SO_2, snow_ice < 0.5, sulfur dioxide total, air mass factor polluted > 0.1, sulfur dioxide total, vertical column > -0.001, qa value > 0.5, cloud fraction crb < 0.3, solar zenith angle < 60. The 15 km-SO_2 band is ingested only when solar zenith angle < 70. For the tropospheric NO_2 column number density, pixels with a qa-value below 75% were filtered and additionally, the qa-value for the ozone was adjusted prior to processing with harpconvert to conform to the following criteria: ozone total vertical column within the range of [0, 0.45]; ozone effective temperature between [180, 260]; ring scale factor within [0, 0.15]; and effective albedo in the range of [-0.5, 1.5] (Atiaga et al. 2023).

For calibration purposes, the average monthly concentrations ($\mu g/m^3$) of the used trace gases were provided by Mexico City automatic air quality monitoring network (RAMA), for its 34 monitoring stations distributed in the metropolitan area. The network follows international standars for measurement and quality control (details about equipment and measured parameters may be found in the following link: https://rama.edomex.gob.mx/que_es_red). The monitoring stations and the RAMA information are provided in Supplementary Material (Table SM1). The period went from December 2019 to October 2020.

Satellite data corresponding to the geographic coordinates of various monitoring stations were extracted from satellite images, and monthly mean data were generated utilizing the appropriate ArcGIS 10.8 tool (Extract Multi Values to Points), which enabled the extraction of cell values for designated locations.

Subsequently, a network of rectangular cells was established in ArcGIS to identify atmospheric sampling points and to extract data at intervals of 5.5 km between points, a parameter determined by the pixel size of the images covering the study areas. In addition to the monthly data analysis, study periods were delineated as occurring before, during, and after the lockdown for each of the cities under investigation (Table 1).

For satellite data validation, level-3 data was from México City and RAMA was used, in the same study period and in the same locations as the monitoring stations. Fit was made by least-squares linear models. As no interaction was expected between treatments (place and period) one way analysis of variance, followed by Tuckey's post-hoc test (Fisher 1992), was used to identify significant differences between mean concentrations for each pair of cities, and period (pre-lockdown, lockdown, and post-lockdown).

Results

Comparison of concentrations between location and period

The areas and the geographic coordinates of the selected cities for the study, which were established through geometric polygons are indicated in Table 1 and Figure SM1.

According to the spatial-temporal analysis, the number of level-3 data selected for NO_2, SO_2 and O_3 were: $n = 8641$ for the Metropolitan District of Quito, $n = 3411$ for Mexico City, $n = 1801$ for the city of Lima and $n = 2498$ for Santiago de Chile. The total number of records per city, including monthly data, was the product of the number of locations by the monthly records in the time series (December 2018 - December 2023).

Comparing the different regions, tropospheric vertical column density (TVCD) values for NO_2 were significantly higher in the city of Santiago de Chile (154 ± 74 µmol/m^2) ($p < 0.05$), followed by the concentrations in the Mexico City (132 ± 59 (µmol/m^2) and Lima City (85 ± 40 µmol/m^2). The lowest concentrations corresponded to the DMQ concentrations (18 ± 8 µmol/m^2) ($p < 0.05$) (Table 3; Fig. 1). The NO_2 densities decreased in all four study cities in the lockdown period, except in Santiago de Chile where it increased significantly ($p < 0.05$) during (131 to 157 µmol/m^2) and after lockdown (162 µmol/m2). In the case of NO_2 concentrations in DMQ, comparing the periods before and after lockdown (17 to 20 µmol/m^2), these also increased significantly, while in the city of Lima the average value decreased from 83 to 75 µmol/m^2, but in Mexico City, no significant variation was observed ($p < 0.05$) (Table 4; Fig. 1).

NO_2 concentrations during the total study period, in the cities of Santiago de Chile and Lima, showed a periodic variation, the highest concentrations were observed especially between the months of June and August, and the lowest during the months of January and February. Whereas, in Mexico City, concentrations in December and January were shown to be significantly higher, and in the months between June and August were the lowest. On average, NO_2 densities in DMQ remained constant during the analyzed period (Fig. 1; Table 2 SM).

On the other hand, the same trend was observed for average SO_2 concentrations: in the DMQ (92 ± 39 µmol/m^2) and the Lima City were found to be significantly lower than in the other study areas (87 ± 19 µmol/m^2) ($p < 0.05$), and the significantly highest SO_2 concentrations ($p < 0.05$) were

Table 3 Trace gas densities in the study areas

Cities	México City $n=208,010$	Lima $n=109,800$	St. Chile $n=152,317$	DMQ $n=527,040$
	Nitrogen dioxide			
Minimun	0	0	8	0
Value (µmol/m^2)	697	311	1359	194
Maximun Value (µmol/m^2)	132±59	85±40	154 ± 74	18±8
Mean +/- standard deviation (µmol/m^2)				
	Sulphur dioxide			
Minimun	0.0	0	0	0
Value (µmol/m^2)	3598	1520	28,616	10,466
Maximun Value (µmol/m^2)	363±85	87±19	727±171	92±39
Mean +/- standard deviation (µmol/m^2)				
	Ozone			
Minimun	100 108 111			104
Value (mmol/m^2)	131 126 144			128
Maximun Value(mmol/m^2)	117±0.34 117±0,28 127±0.39			114±0,65
Mean +/- standard deviation (mmol/m^2)				

found in the city of Santiago de Chile (727 ± 171 µmol/m^2) ($p>0.05$) (Table 3; Fig. 1).

When compared the conditions of all periods, the average SO_2 densities showed irregular variations among the different study areas for the different periods. In the DMQ and the Mexico City, there was a significantly decrease in the lockdown period: (41 to 40 µmol/m^2) and (334 to 293 µmol/m^2), respectively, however after lockdown, SO_2 concentrations increased in both cities, in the DMQ approximately threefold, from values close to 40 umol/m^2 to around 126 umol/m^2 and in Mexico City to 293 umol/m^2. In Santiago de Chile, concentrations before and after lockdown were shown to be significantly lower ($p<0.05$) than those in the lockdown period. Whereas, in the city of Lima for the three periods: before, during, and after lockdown, significant increase in concentrations were observed (Table 4; Fig. 1).

Satellite images corresponding to monthly mean SO_2 values (Table 3 SM, Fig. 2), showed irregular variations in SO_2 concentrations among the different cities for the different months within the study period. Likewise, significantly higher concentrations are observed ($p\leq 0.05$) in the months of June and July, and the lowest in the months of December and January in Santiago de Chile; for the cities of Lima, Mexico and DMQ, no significant variations were observed during the whole study period ($p>0.05$).

Ozone concentrations in Santiago de Chile were also significantly higher ($p<0.05$) than in the cities of Mexico, Lima and DMQ. Likewise, in the cities of Santiago, Lima and DMQ a decrease in these concentrations was observed during the Lockdown, while in the Mexico City, ozone densities increased significantly.

Discussion of results

Trace gas densities from the Latin American cities were significantly different, the highest concentrations were observed in Santiago and Mexico City. These results are consistent, since both cities are among the most urbanized regions in the world. These urbanization processes bring negative effects as road congestion and pollution (Bedoya-Maya et al. 2022). Furthermore, Santiago and Mexico are among the thirty most congested cities of the world (Bedoya-Maya et al. 2022) and Chile holds eight of the 15 most polluted cities in Latin America and the Caribbean (Villacura et al. 2024). Despite the implementation of several measures to control and prevent air pollution in cities such as Santiago and Mexico City (Vega et al. 2021; Villacura et al. 2024), Santiago showed the highest concentrations of the studied atmospheric gases ($p<0.05$) compared to Mexico City, Lima and the Metropolitan District of Quito, while Mexico City was once the most polluted megacity worldwide (Vega et al. 2021). In this study, in Mexico City the satellite densities were found to be significantly lower ($p<0.05$) than Santiago de Chile.

On the other hand, NO_2 concentrations decreased during lockdown in all study cities (Mexico City: 56%, Lima City: 76% and DMQ: 70%), except in Santiago, where there was an increment of 20%, this may be due to, as in the majority of cities of Chile, Santiago has thermal inversions during winter months (April-August), which make the atmospheric conditions impede the dispersion of pollutants (Garcia-Chevesich et al. 2014). Thus, the monthly average variation of the NO_2 concentration in Santiago de Chile (Fig. 2) during the whole study period, showed an increase in the NO_2 concentrations since April, showing the highest values in July and August. However, even though in the city of Santiago the periodicity is maintained in the different years, a decrease in concentrations is observed in 2020 and in 2023, in this last year it may be due to the adopted measures to reduce the air pollution. In Mexico City, the variation of NO_2 concentrations is also periodic, whose highest values

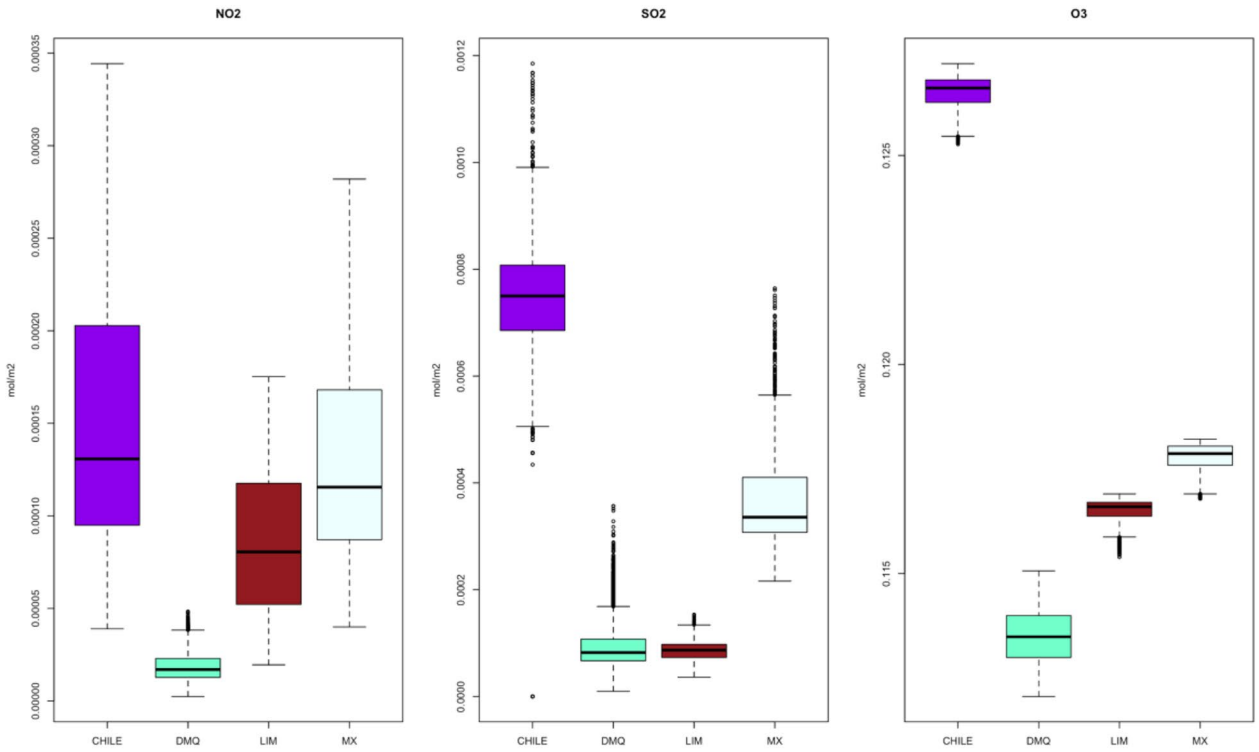

a)

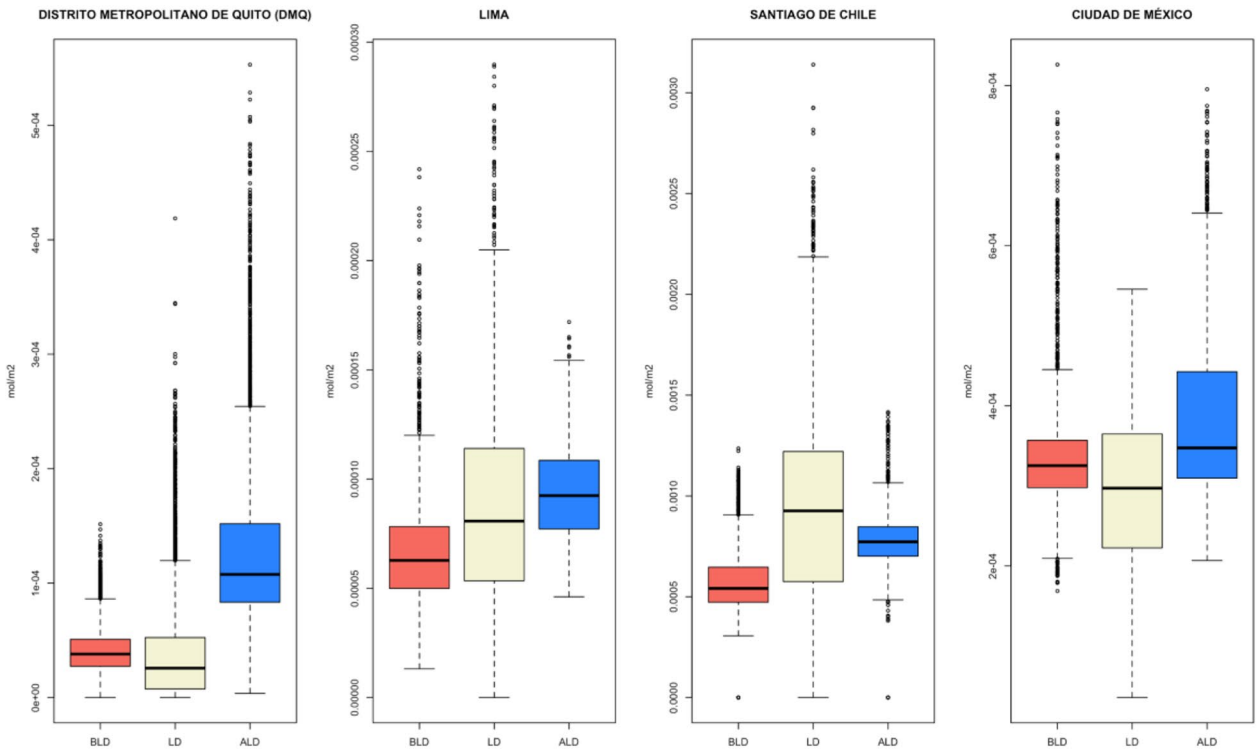

b)

Fig. 1 (**a**) Averaged tropospheric NO_2, SO_2, and O_3 total column densities in the studied cities, during the period between December 2018– December 2023. (**b**) Comparison of NO_2 column densities for the period before the lockdown (BLD), during (LD) and the after the lockdown (ALD)

Table 4 Trace gas densities in cities of America Latina during the periods (mean +/- standard deviation)

City	Before Lockdown	Lockdown	After Lockdown	
	Nitrogen dioxide (µmol/m^2)			% change post to pre lockdown
Mexico City n=3411	133±62	85 ± 34	135 ± 60	+1.5%*
DMQ n=8641	17 ± 7	10±6	20 ± 6	+17%*
Lima n=1801	83±42	47±22	75 ± 45	-9.6%*
Santiago n=2498	131±61	157±73	162±80	24%*
	Sulphur dioxide (µmol/m^2)			
Ciudad de Mexico n=3411	334±70	293±97	377±99	+13*
DMQ n=8641	41±20	40±46	126±74	+207%*
Lima n=1801	68±29	88±48	93±28	+37%*
Santiago de Chile n=2498	565±188	960±507	759±190	+34%*
	Ozone (mmol/m^2)			
Ciudad de Mexico n=3411	113±0.3	120±0.6	119±0.3	5.3%*
DMQ n=8641	112±0.6	111±0.5	114±0.6	1.8%**
Lima n=1801	114±0.2	112±0.3	116±0.3	1.8%**
Santiago de Chile n=2498	125±0.4	120 ± 0.3	128±2.6	2.4%*

*: significant difference; **: non-significant difference. See text for details

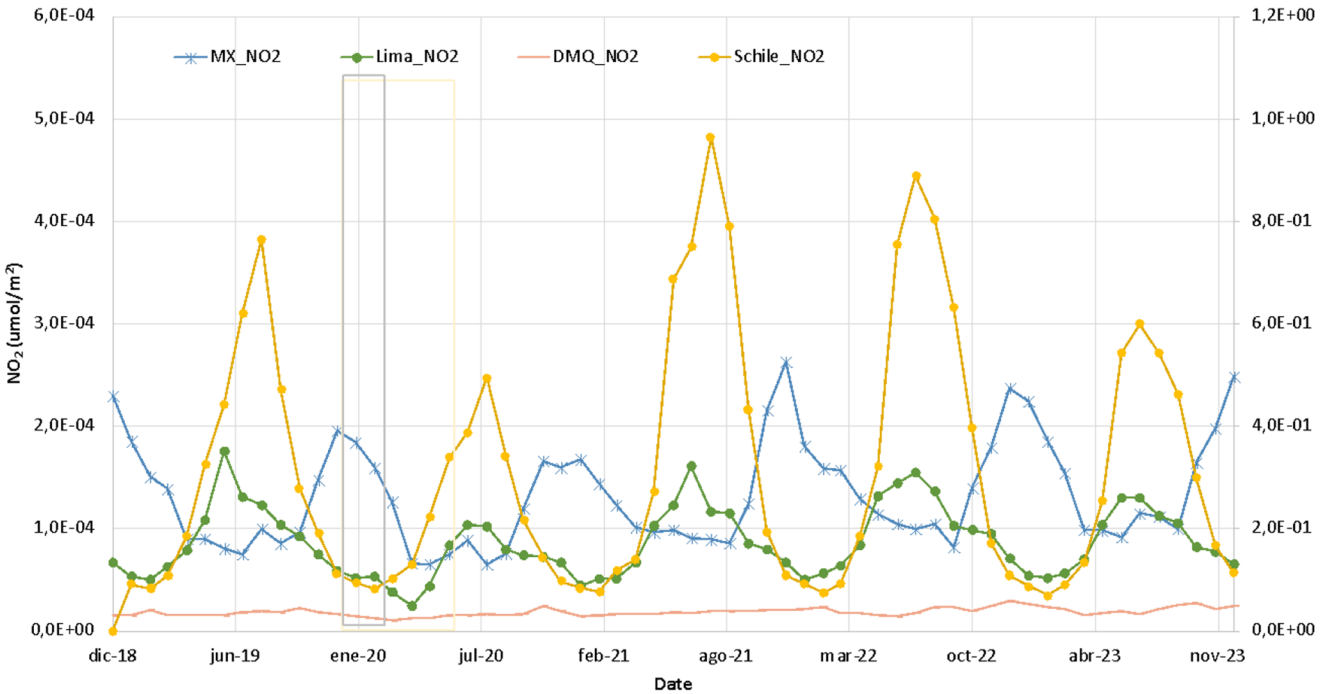

Fig. 2 TROPOMI spatially averaged monthly tropospheric NO_2 column densities for each of the studied cities. Lockdown period is indicated by the grey box

correspond to December and January, it may be due to the increase in traffic because of the Christmas holidays.

Latin American cities have also recorded reduction in SO_2 concentrations during the lockdowns. In Mexico City, showed a decrease of 14%. In DMQ, reductions have been smaller than in Mexico City: 2.5%. In contrast, Santiago and Lima showed an increase of 70% and 29%, respectively. The high concentrations in Santiago, which could be also explained by thermal inversions during winter.

As for O_3, in Santiago, DMQ and Lima City, densities decreased by 4%, 0,9% and 1,7%, respectively. In contrast, Mexico city showed an increase of O_3 of 6% on average. This behavior of the O_3, significant decrease in Santiago de Chile and significant increase in Mexico City, can be explained by the fact that the decrease in NO_2, one of its precursor compounds, leads to the accumulation of O_3 (Rathod et al. 2021; Toro A. et al. 2021; Atiaga et al. 2023). In contrast, the NO_2 increase, which reacts with ozone, would possibly reduce the concentrations of ozone, according to following reactions:

$$NO_2 + h\gamma \rightarrow NO + O \quad (1)$$

$$O + O_2 + M \rightarrow O_3 + M \quad (2)$$

$$NO + O_3 \rightarrow NO_2 + O \quad (3)$$

$$VOCs + OH \rightarrow RO_2 + H_2O \quad (4)$$

$$RO_2 + NO \rightarrow RO + NO_2 \quad (5)$$

Equation 3 indicates ozone consumption by NO_x: when NO_x concentration decreases, ozone concentration increases (Cazorla et al. 2021; Rathod et al. 2021; Zhao et al. 2021; Atiaga et al. 2023). When VOC concentrations remain constant or do not decrease significantly, ozone concentrations increase when the available NOx is insufficient to consume ozone (Pei et al. 2020; Cazorla et al. 2021).

The influence of local meteorological conditions on pollutant levels in the studied cities during and after the lockdown period was significant and varied by location. In Santiago de Chile, winter thermal inversions (April–August) trapped pollutants near the surface, overriding emission reductions during lockdowns. This led to unexpected increases in NO_2 and SO_2 concentrations during lockdown and post-lockdown periods, as stagnant air hindered dispersion. Similarly, post-lockdown SO_2 spikes in Santiago were exacerbated by these inversions, highlighting the need for seasonal emission controls targeting industrial and vehicular sources during inversion-prone months.

In Mexico City, the valley topography and high-altitude limited pollutant dispersion, while seasonal traffic peaks (e.g., December holidays) drove periodic NO_2 increases. During lockdown, reduced NO_2 emissions altered ozone chemistry: lower NOx levels diminished the titration effect (where NO consumes ozone), enabling O_3 accumulation. Post-lockdown, rebounding NO_2 levels partially suppressed O_3, but the interplay with volatile organic compounds (VOCs) and persistent valley effects underscored the need for dual NOx-VOC reduction strategies. Lima's coastal winds channeled pollutants inland, where mountainous terrain trapped emissions. Despite lockdown-driven emission drops, this dynamic limited improvements, and post-lockdown SO_2 increases reflected resumed industrial activity under unchanged wind patterns. Quito's narrow, steep valleys concentrated vehicle emissions in lower zones. Post-lockdown SO_2 tripling signaled industrial reactivation in topographically constrained areas, emphasizing the role of local wind circulation and elevation in pollutant accumulation.

Comparing ozone concentrations in the pre-lockdown and post-lockdown periods, an increase in these concentrations was observed in all study cities, between 1,8% and 5,3% (Table 4). On the other hand, in a study carried out in some provinces of Ecuador, where total column ozone densities were related to tropospheric column ozone densities, the same upward trend was observed in the two data series (Atiaga et al. 2023).

In addition, we examined the correlation (Figure SM2) between column density data for NO_2, O_3, and SO_2 and the surface concentrations from RAMA monitoring stations. Similar variations in concentrations were observed for NO_2 (Fig. 3), showing an average regression coefficient of approximate 0.9 (Pearson and Spearman). In the case of SO_2 (Figure SM3), no significant correlations were found (-0.17 Pearson, -0.022 Spearman) and 0.58 (Pearson and Spearman) for ozone, where similar variations were observed in the two data series (Figure SM4).

In the case of NO_2, the correlation between satellite and ground measurements has been studied in numerous researches (Baldasano 2020; Rathod et al. 2021; Ghasempour et al. 2021; Atiaga et al. 2023; Mahmud et al. 2023). The high regression coefficient can be attributed to two reasons: NO_2 absorbs strongly in the 425–450 nm absorption window where few other species absorb and NO_2 also has a short lifespan of 2–24 h, making adjustment easier and retrieve column counts (Potts et al. 2024).

The observed post-lockdown increases in NO_2 and SO_2 concentrations necessitate urban air quality management frameworks that address both emission source dynamics and site-specific environmental parameters. In Santiago de Chile, persistent elevated NO_2 concentrations during and after mobility restriction periods were associated with winter thermal inversion phenomena, indicating that temporally-targeted emission control protocols, namely vehicular movement restrictions and industrial output limitations, during inversion-susceptible periods, may attenuate pollution maxima. Quito's threefold increase in SO_2 concentrations following restriction cessation demonstrates pollution rebound effects concurrent with economic activity resumption, suggesting requirements for enhanced industrial emission standards and implementation of low-emission energy infrastructure.

The integration of satellite-derived atmospheric composition data, validated through ground-based monitoring networks, provides a resource-efficient methodology for air quality surveillance and regulatory effectiveness assessment, particularly valuable in regions with limited monitoring infrastructure.

These results highlight the diverse impacts of lockdowns on air quality, with reductions in certain pollutants and increases in others, emphasizing the complex relationship between human activity and air quality. They show how short-term alterations in mobility and industry affect pollutant levels, potentially guiding policymakers in creating sustainable urban areas, alleviating pollution, and safeguarding public health.

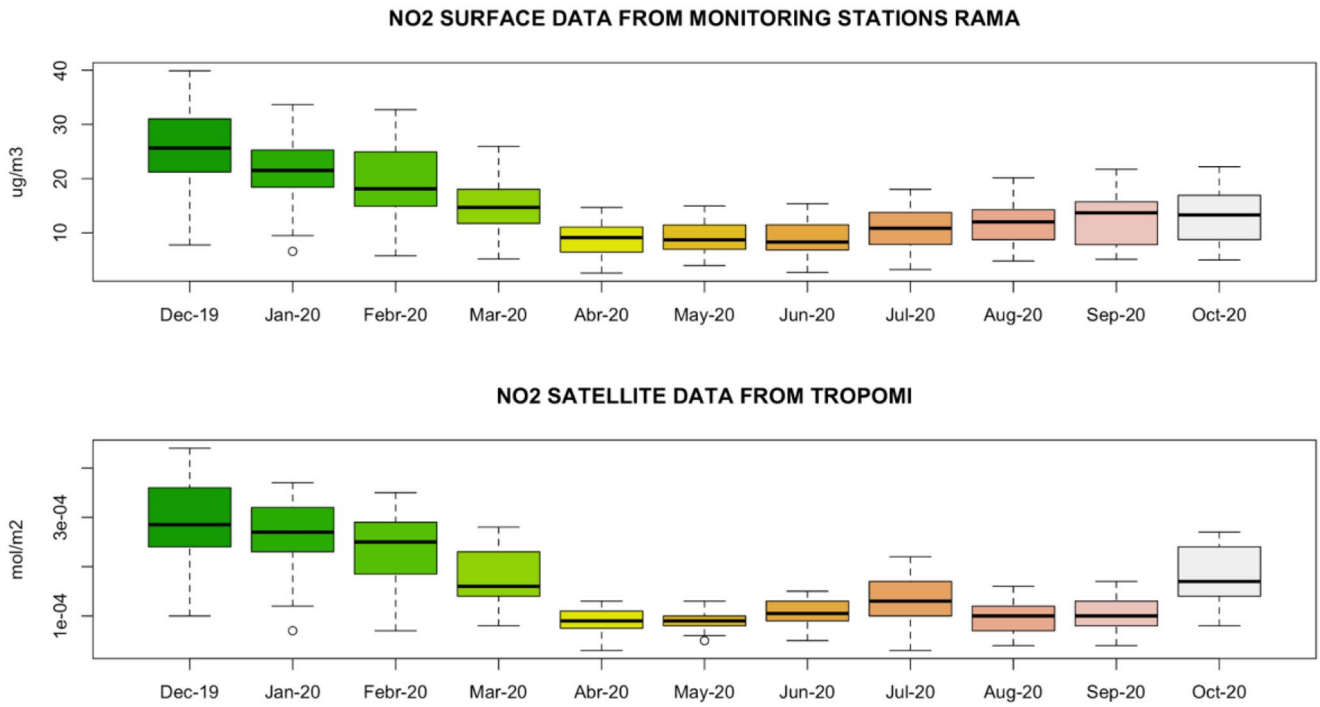

Fig. 3 Monthly variation of NO_2 surface concentrations measured at soil level (RAMA monitoring network) (top), and NO_2 tropospheric column densities during the period December 2019 - October 2020, determined from satellite data (bottom)

Methodological limitations of satellite-based air quality assessment

The study's reliance on satellite data presents notable limitations, particularly regarding spatial resolution and environmental interference. Sentinel-5P's ~ 5.5 km resolution may miss localized pollution hotspots in topographically complex cities like Quito or Mexico City, where emissions vary sharply over short distances. Cloud cover, aerosols, and sensor cross-sensitivities (e.g., spectral overlaps affecting SO_2 retrievals) introduce inaccuracies, despite quality filters. Weak correlations between satellite and ground data for SO_2 (Pearson: -0.17) highlight detection challenges, compounded by the mismatch between satellite column densities and ground-level surface measurements. Temporal gaps further limit validation, as ground data for cities like Lima or Santiago were sparse or confined to short periods, while satellite data spanned 2018–2023.

Environmental factors, such as Santiago's thermal inversions and Lima's coastal winds, mediated pollutant dispersion in ways satellite data alone could not fully resolve. Additionally, the focus on four cities restricts generalizability to regions with differing emission profiles. These limitations underscore the need for hybrid approaches: integrating higher-resolution ground networks, advanced modeling, and sensor-specific error corrections to improve reliability. Future studies should prioritize expanding validation across diverse urban settings to enhance satellite-derived air quality assessments and inform adaptive policies.

Conclusion

This study investigated spatiotemporal variations in NO_2, SO_2, and O_3 concentrations across four major Latin American cities, namely Mexico City, Lima, Santiago de Chile, and Quito, utilizing Sentinel-5P satellite data and ground-based monitoring stations. Our analysis spanned a period encompassing pre-lockdown, lockdown, and post-lockdown phases associated with the COVID-19 pandemic, enabling a multifaceted assessment of pollutant behavior under varying conditions.

Results revealed significant spatial heterogeneity in pollutant concentrations. Santiago consistently exhibited the highest levels of NO_2 and SO_2, significantly exceeding those observed in other study areas. This disparity underscores the need for targeted air quality management strategies within Santiago, considering its unique geographical characteristics and urban development patterns. Mexico City showed high NO_2 concentrations, but lower than Santiago. In contrast, Quito exhibited the lowest concentrations of both pollutants.

The COVID-19 lockdowns resulted in diverse responses. While NO_2 concentrations decreased across most cities (except for Santiago), SO_2 showed more complex behavior.

Santiago demonstrated an increase in SO_2 during lockdown, which may be attributed to meteorological factors such as thermal inversions. This highlights the importance of considering local climatological conditions when assessing the impact of interventions on air quality. Ozone concentrations showed a general decrease during the lockdown period, yet with increase in Mexico City post-lockdown.

The comparison of satellite data with ground-based monitoring station data revealed strong correlations for NO_2, validating the use of satellite data as a cost-effective complement to ground-based monitoring networks, especially in resource-constrained settings. These results are particularly valuable for developing nations seeking to enhance their air quality monitoring capabilities without incurring extensive infrastructural investments.

The study shows the effectiveness of integrating satellite data into air quality assessments, highlighting spatial and temporal variations of key pollutants across diverse urban environments in Latin America. It underscores the need for city-specific interventions, tailored to unique geographic and climatic factors, to effectively mitigate air pollution and improve public health. Subsequent investigations may explore multi-sensor integration methodologies, combining Sentinel-5P data with ground-based LiDAR systems or unmanned aerial vehicle (UAV) instrumentation to enhance spatial resolution and measurement accuracy. Machine learning algorithms could be developed for identification of statistical anomalies in temporal pollution patterns, enabling early detection of emerging air quality concerns. Longitudinal epidemiological studies examining correlations between observed air quality fluctuations and population health outcomes would provide critical data for evidence-based policy formulation and public health intervention strategies.

Supplementary Information The online version contains supplementary material available at https://doi.org/10.1007/s11869-025-01738-z.

Author contributions All authors contributed to the study conception and design. Material preparation, data collection and analysis were performed by Páez Fernando, Wilson Jácome, Castro Rafael, Collahuazo Edison, Luís Miguel Nunes. The first draft of the manuscript was written by Oliva Atiaga and all authors commented on previous versions of the manuscript. All authors read and approved the final manuscript.

Funding Open access funding provided by FCT|FCCN (b-on).
This work was supported by Universidad de las Fuerzas Armadas-ESPE of Ecuador through Project 2021-PIC-001-CTE.

Data availability The datasets generated and analyzed during the current study are available in the Github repository,https://github.com/owid/covid-19-data/tree/master/public/data.

Declarations

Ethics approval and consent to participate Not applicable.

Consent for publication All authors agree with the publication.

Competing interests The authors have no relevant financial or non-financial interests to disclose.

References

Albayati N, Waisi B, Al-Furaiji M et al (2021) Effect of COVID-19 on air quality and pollution in different countries. J Transp Health 21:101061. https://doi.org/10.1016/j.jth.2021.101061

Anenberg SC, Bindl M, Brauer M et al (2020) Using satellites to track indicators of global air pollution and climate change impacts: lessons learned from a NASA-Supported Science-Stakeholder collaborative. https://doi.org/10.1029/2020GH000270. GeoHealth 4:e2020GH000270

Atiaga O, Guerrero F, Páez F et al (2023) Assessment of variations in air quality in cities of Ecuador in relation to the lockdown due to the COVID-19 pandemic. Heliyon 9:e17033. https://doi.org/10.1016/j.heliyon.2023.e17033

Baldasano JM (2020) COVID-19 lockdown effects on air quality by NO2 in the cities of Barcelona and Madrid (Spain). Sci Total Environ 741:140353. https://doi.org/10.1016/j.scitotenv.2020.140353

Bedoya-Maya F, Calatayud A, González Mejía V (2022) Estimating the effect of road congestion on air quality in Latin America. Transp Res Part D: Transp Environ 113:103510. https://doi.org/10.1016/j.trd.2022.103510

Benchrif A, Wheida A, Tahri M et al (2021) Air quality during three covid-19 lockdown phases: AQI, PM2.5 and NO2 assessment in cities with more than 1 million inhabitants. Sustainable Cities Soc 74:103170. https://doi.org/10.1016/j.scs.2021.103170

Bodah BW, Neckel A, Stolfo Maculan L et al (2022) Sentinel-5P TROPOMI satellite application for NO2 and CO studies aiming at environmental valuation. J Clean Prod 357:131960. https://doi.org/10.1016/j.jclepro.2022.131960

Brooks R, Harris B (2023) The US Recovery from COVID-19 in International Comparison. Brookings Institution, Washington, D.C., https://www.brookings.edu/articles/the-us-recovery-from-covid-19-in-international-comparison/

Burns J, Boogaard H, Polus S et al (2020) Interventions to reduce ambient air pollution and their effects on health: an abridged Cochrane systematic review. Environ Int 135:105400. https://doi.org/10.1016/j.envint.2019.105400

Cazorla M, Herrera E, Palomeque E, Saud N (2021) What the COVID-19 lockdown revealed about photochemistry and

Ozone production in Quito, Ecuador. Atmospheric Pollution Res 12:124–133. https://doi.org/10.1016/j.apr.2020.08.028
Crosman E (2021) Meteorological drivers of permian basin methane anomalies derived from TROPOMI. Remote Sensing 13: 896.https://doi.org/10.3390/rs13050896
Fisher RA (1992) Statistical methods for research workers. In: Kotz S, Johnson NL (eds) Breakthroughs in statistics: methodology and distribution. Springer, New York, NY, pp 66–70
Garcia-Chevesich PA, Alvarado S, Neary DG et al (2014) Respiratory disease and particulate air pollution in Santiago Chile: contribution of erosion particles from fine sediments. Environ Pollut 187:202–205. https://doi.org/10.1016/j.envpol.2013.12.028
Ghasempour F, Sekertekin A, Kutoglu SH (2021) Google Earth engine based spatio-temporal analysis of air pollutants before and during the first wave COVID-19 outbreak over Turkey via remote sensing. J Clean Prod 319:128599. https://doi.org/10.1016/j.jclepro.2021.128599
Gómez Peláez LM, Santos JM, de Almeida Albuquerque TT et al (2020) Air quality status and trends over large cities in South America. Environ Sci Policy 114:422–435. https://doi.org/10.1016/j.envsci.2020.09.009
Gorelick N, Hancher M, Dixon M et al (2017) Google Earth engine: Planetary-scale Geospatial analysis for everyone. Remote Sens Environ 202:18–27. https://doi.org/10.1016/j.rse.2017.06.031
Ialongo I, Virta H, Eskes H, Hovila J, Douros J (2020) Comparison of TROPOMI/Sentinel-5 precursor NO2 observations with ground-based measurements in Helsinki. Atmos Meas Tech 13:205–218. https://doi.org/10.5194/amt-13-205-2020
Levelt PF, Joiner J, Tamminen J et al (2018) The Ozone monitoring instrument: overview of 14 years in space. Atmos Chem Phys 18:5699–5745. https://doi.org/10.5194/acp-18-5699-2018
Li X, Hussain SA, Sobri S, Md Said MS (2021) Overviewing the air quality models on air pollution in Sichuan basin, China. Chemosphere 271:129502. https://doi.org/10.1016/j.chemosphere.2020.129502
Mahmud K, Mitra B, Uddin MS et al (2023) Temporal assessment of air quality in major cities in Nigeria using satellite data. Atmospheric Environment: X 20:100227. https://doi.org/10.1016/j.aeaoa.2023.100227
Mathys T, de Souza FT, Barcellos Dda, Molderez S I (2023) The relationship among air pollution, meteorological factors and COVID-19 in the Brussels capital region. Sci Total Environ 857:158933. https://doi.org/10.1016/j.scitotenv.2022.158933
Pei Z, Han G, Ma X et al (2020) Response of major air pollutants to COVID-19 lockdowns in China. Sci Total Environ 743:140879. https://doi.org/10.1016/j.scitotenv.2020.140879
Potts DA, Ferranti EJS, Hey JDV (2024) Investigating the barriers and pathways to implementing satellite data into air quality monitoring, regulation and policy design in the united Kingdom. Environ Sci Policy 151:103621. https://doi.org/10.1016/j.envsci.2023.103621
Rathod A, Sahu SK, Singh S, Beig G (2021) Anomalous behaviour of Ozone under COVID-19 and explicit diagnosis of O3-NOx-VOCs mechanism. Heliyon 7:e06142. https://doi.org/10.1016/j.heliyon.2021.e06142
Ray RL, Singh VP, Singh SK et al (2022) What is the impact of COVID-19 pandemic on global carbon emissions? Sci Total Environ 816:151503. https://doi.org/10.1016/j.scitotenv.2021.151503
Rojas JP, Urdanivia FR, Garay RA et al (2021) Effects of COVID-19 pandemic control measures on air pollution in Lima metropolitan area, Peru in South America. Air Qual Atmos Health 14:925–933. https://doi.org/10.1007/s11869-021-00990-3
Romero Y, Chicchon N, Duarte F et al (2020) Quantifying and Spatial disaggregation of air pollution emissions from ground transportation in a developing country context: case study for the Lima metropolitan area in Peru. Sci Total Environ 698:134313. https://doi.org/10.1016/j.scitotenv.2019.134313
Sahraei MA, Kuşkapan E, Çodur MY (2021) Public transit usage and air quality index during the COVID-19 lockdown. J Environ Manage 286:112166. https://doi.org/10.1016/j.jenvman.2021.112166
Shikwambana L, Mhangara P, Mbatha N (2020) Trend analysis and first time observations of sulphur dioxide and nitrogen dioxide in South Africa using TROPOMI/Sentinel-5 P data. Int J Appl Earth Obs Geoinf 91:102130. https://doi.org/10.1016/j.jag.2020.102130
Toro AR, Catalán F, Urdanivia FR et al (2021) Air pollution and COVID-19 lockdown in a large South American City: Santiago metropolitan area, Chile. Urban Clim 36:100803. https://doi.org/10.1016/j.uclim.2021.100803
United Nations (2019) World Population Prospects 2019| Population Division. In: The 2019 revision of the World Population Prospects. https://www.un.org/development/desa/pd/news/world-population-prospects-2019-0. Accessed 21 Jan 2025
Veefkind JP, Aben I, McMullan K et al (2012) TROPOMI on the ESA Sentinel-5 precursor: A GMES mission for global observations of the atmospheric composition for climate, air quality and Ozone layer applications. Remote Sens Environ 120:70–83. https://doi.org/10.1016/j.rse.2011.09.027
Vega E, Namdeo A, Bramwell L et al (2021) Changes in air quality in Mexico City, London and Delhi in response to various stages and levels of lockdowns and easing of restrictions during COVID-19 pandemic. Environ Pollut 285:117664. https://doi.org/10.1016/j.envpol.2021.117664
Villacura L, Sánchez LF, Catalán F et al (2024) An overview of air pollution research in Chile: bibliometric analysis and scoping review, challenger and future directions. Heliyon 10. https://doi.org/10.1016/j.heliyon.2024.e25431
Volke MI, Abarca-del-Rio R, Ulloa-Tesser C (2023) Impact of mobility restrictions on NO2 concentrations in key Latin American cities during the first wave of the COVID-19 pandemic. Urban Clim 48:101412. https://doi.org/10.1016/j.uclim.2023.101412
Vu BN, Tapia V, Ebelt S et al (2021) The association between asthma emergency department visits and satellite-derived PM2.5 in Lima, Peru. Environ Res 199:111226. https://doi.org/10.1016/j.envres.2021.111226
Wang Q, Li S (2021) Nonlinear impact of COVID-19 on pollutions–Evidence from Wuhan, new York, Milan, Madrid, Bandra, London, Tokyo and Mexico City. Sustainable Cities Soc 65:102629. https://doi.org/10.1016/j.scs.2020.102629
World Health Organization (2025) Air pollution. In: Air pollution. https://www.who.int/health-topics/air-pollution. Accessed 21 Jan 2025
Zalakeviciute R, Bonilla Bedoya S, Mejia Coronel D et al (2024) Central parks as air quality oases in the tropical Andean City of Quito. Atmospheric Environment: X 21:100239. https://doi.org/10.1016/j.aeaoa.2024.100239
Zhao F, Liu C, Cai Z et al (2021) Ozone profile retrievals from TROPOMI: implication for the variation of tropospheric Ozone during the outbreak of COVID-19 in China. Sci Total Environ 764:142886. https://doi.org/10.1016/j.scitotenv.2020.142886